npg

Open

ORIGINAL ARTICLE

Platelets generated from human embryonic stem cells are functional *in vitro* and in the microcirculation of living mice

Shi-Jiang Lu[1, 3, *], Feng Li[1, 3, *], Hong Yin[1], Qiang Feng[1, 3], Erin A Kimbrel[1, 3], Eunsil Hahm[2], Jonathan N Thon[5], Wei Wang[1], Joseph E Italiano[5], Jaehyung Cho[2], Robert Lanza[1, 4]

[1]*Stem Cell and Regenerative Medicine International, 33 Locke Drive, Marlborough, MA 01752, USA;* [2]*Department of Pharmacology and Anesthesiology, University of Illinois at Chicago, 835 South Wolcott Avenue, Chicago, IL 60612, USA;* [3]*Department of Applied Bioscience, Cha University, Seoul, Korea;* [4]*Advanced Cell Technology, 33 Locke Drive, Marlborough, MA 01752, USA;* [5]*Vascular Biology Program, Department of Surgery, Children's Hospital, and Division of Hematology, Brigham and Women's Hospital, Harvard Medical School, 1 Blackfan Circle, Boston, MA 02115, USA*

Platelets play an essential role in hemostasis and atherothrombosis. Owing to their short storage time, there is constant demand for this life-saving blood component. In this study, we report that it is feasible to generate functional megakaryocytes and platelets from human embryonic stem cells (hESCs) on a large scale. Differential-interference contrast and electron microscopy analyses showed that ultrastructural and morphological features of hESC-derived platelets were indistinguishable from those of normal blood platelets. In functional assays, hESC-derived platelets responded to thrombin stimulation, formed microaggregates, and facilitated clot formation/retraction *in vitro*. Live cell microscopy demonstrated that hESC-platelets formed lamellipodia and filopodia in response to thrombin activation, and tethered to each other as observed in normal blood. Using real-time intravital imaging with high-speed video microscopy, we have also shown that hESC-derived platelets contribute to developing thrombi at sites of laser-induced vascular injury in mice, providing the first evidence for *in vivo* functionality of hESC-derived platelets. These results represent an important step toward generating an unlimited supply of platelets for transfusion. Since platelets contain no genetic material, they are ideal candidates for early clinical translation involving human pluripotent stem cells.

Introduction

Platelets play a critical role in stimulating clot formation and repair of vascular injury. However, because of their short life span of only 7-10 days, platelets constantly need to be replaced in order to maintain normal levels (150-400 × 10^3/μl) in the blood. Life-threatening

*These two authors contributed equally to this work.
Correspondence: Shi-Jiang Lu[a], Jaehyung Cho[b], Robert Lanza[c]
[a]Tel: +508-791-0305 ext 684
E-mail: jlu@steminternational.com
[b]Tel: +312-355-5923
E-mail: thromres@uic.edu
[c]Tel: +508-756-1212 ext 315
E-mail: rlanza@advancedcell.com
Received 30 November 2010; revised 12 December 2010; accepted 13 December 2010; published online 11 January 2011

thrombocytopenia (low platelet counts, generally < 10-30 × 10^3/μl) can occur in patients for a variety of reasons, including chemotherapy, radiation treatment, or organ transplant surgery. To circumvent risks associated with these conditions, platelet transfusions have become a mainstay therapy; yet high demand and limited shelf life have created a constant shortage in transfusion supplies [1]. The ability to generate HLA-matched platelets *in vitro* would provide significant advantages over currently used donor-dependent programs.

Platelet production *in vivo* is a highly efficient process with 2 000-10 000 platelets being produced from each megakaryocyte (MK) precursor cell [2, 3]. Signaling through thrombopoietin (TPO) and other cytokines in the bone marrow (BM), such as interleukin (IL)-3, IL-6, IL-9, IL-11, bone morphogenetic protein (BMP)-4, flt3 ligand (FL), and stem cell factor (SCF) is thought

to facilitate MK maturation and platelet production [4], while transcription factors, such as GATA-1 and FOG-1, are thought to help orchestrate the progressive lineage commitment, maturation, and fragmentation of MKs into platelets [5-7]. MK maturation involves the acquisition of characteristic cell surface markers, such as glycoprotein (GP) IIb/IIIa (CD41, also known as integrin αIIbβ3, a receptor for fibrinogen), GPIb (CD42b/c), GPIX (CD42a), and GPV (CD42d), several rounds of endomitosis, and the accumulation of components necessary for platelet biogenesis such as α- and dense-granules, and proteins such as von Willebrand factor (vWF) and platelet factor 4 (PF4) [8, 9]. Cumulatively, these changes result in the generation of large polyploid MKs that are 50-100 microns in diameter, up to 64N in DNA content, and primed for thrombopoiesis, i.e., the assembly and release of platelets into the blood stream (reviewed by Kosaki [10] and Patel *et al.* [11]).

Success has been achieved in producing functional MKs and platelets from CD34+ hematopoietic cells of the BM, cord blood, and peripheral blood (PB) *in vitro* [12, 13]. However, these cells are unable to alleviate the ongoing need for donors because of their limited *in vitro* expansion capabilities. In contrast, human embryonic stem cells (hESCs) can be propagated *in vitro* indefinitely, providing a potentially unlimited and donorless source of cells for therapeutic purposes. Although two studies [14, 15] have provided a proof of principle for *in vitro* production of hESC-derived MKs, only one of them [15] extended their studies to include the subsequent production of platelets. Despite this pioneering work, the low yields of hESC-MKs, labor-intensive methodologies, and limited *in vitro* functionality testing of hESC-platelets left critical questions unanswered: (1) can hESC-derived MKs and platelets be produced on a clinically relevant scale, and (2) are these platelets functional upon transfusion into a living animal?

In this study, we describe an efficient method of gen-erating functional MKs from hESCs on a large scale using hemangioblasts/blast cells (BCs) as intermediates [16, 17]. Platelets produced from hESC-derived MKs displayed all of the ultrastructural and morphological criteria that are typical of blood platelets, and possessed characteristic properties of functional platelets, such as activation by thrombin, spreading on fibrinogen- and vWF-coated surfaces, and formation/retraction of fibrin clots. Importantly, fluorescence intravital microscopy studies demonstrated that hESC-derived platelets incorporated into developing mouse platelet thrombi at sites of laser-induced arteriolar wall injury in a manner and degree similar to that observed for normal human blood platelets. These results provide valuable evidence that hESC-derived platelets may be useful for platelet transfusion.

Results

Large-scale generation of MKs from hESC-derived hemangioblasts/BCs

Our previous studies have shown that hemangioblasts/BC derived from hESCs can efficiently differentiate into erythroid cells [18]. Since MKs and erythrocytes share a common progenitor during mammalian hematopoiesis, we performed a series of experiments to determine whether hESC-derived BCs could also be induced to differentiate into MKs. BCs harvested from day 6 to day 8 cultures were first tested for their megakaryopoietic potential using a colony-forming unit (CFU)-MK assay. Within 10-12 days of plating in Megacult-C media, BCs derived from all three tested hESC lines (HuES-3, MA01, and MA09) developed CFU-MK colonies and stained positive for CD41, with cellular processes resembling proplatelets extending from some of the CD41+ cells (Supplementary information, Figure S1).

To determine which cytokines and growth factors are required for BCs to differentiate into MKs, we tested

Figure 1 Generation and characterization of megakaryocytes (MKs) derived from human embryonic stem cells (hESCs). **(A)** Numbers of CD41a+ cells generated from 8 × 10⁴ hemangioblasts/blast cells derived from hESCs after 4-6 day culture in Stemline II medium supplemented with TPO (50 ng/ml) or TPO (50 ng/ml) plus SCF (20 ng/ml). ***$P < 0.001$, $n = 4$. **(B)** Average numbers of CD41a+ cells generated at different days. Blast cells were plated in Stemline II medium supplemented with TPO (50 ng/ml), SCF (20 ng/ml) and IL-11 (20 ng/ml), CD41a+ cells from four experiments were analyzed by flow cytometry. **(C)** Flow cytometry analyses of blast cells (day 0 MK culture, left panel), and cells from day 4 MK cultures show the expression of CD41a and CD235a (middle panel), and CD41a and CD42b (right panel) antigens. **(D)** Average size (diameter) of cells at the beginning (19.0 ± 4.2 μm, $n = 111$) and 6 days (25.6 ± 12.5 μm, $n = 124$) after MK culture. Cells were measured from digital images of Giemsa-stained cells. ***$P < 0.001$. **(E)** DNA ploidy analysis by flow cytometry of CD41a+ cells. DNA ploidy up to 32N was observed in these cells. **(F)** Giemsa staining of cells from day 6 MK culture. **(G)** Immunofluorescence of von Willebrand factor (vWF, red) and CD41 (green) proteins in cells from day 6 MK culture. vWF is localized in the cytoplasm in a punctate pattern, which is typical for MKs. CD41 is expressed on the surface. DAPI (blue) stain shows polynuclei (polyploidy). **(H)** A representative phase contrast image shows the pro-platelet forming MKs in day 4 cultures. Bars = 20 μm.
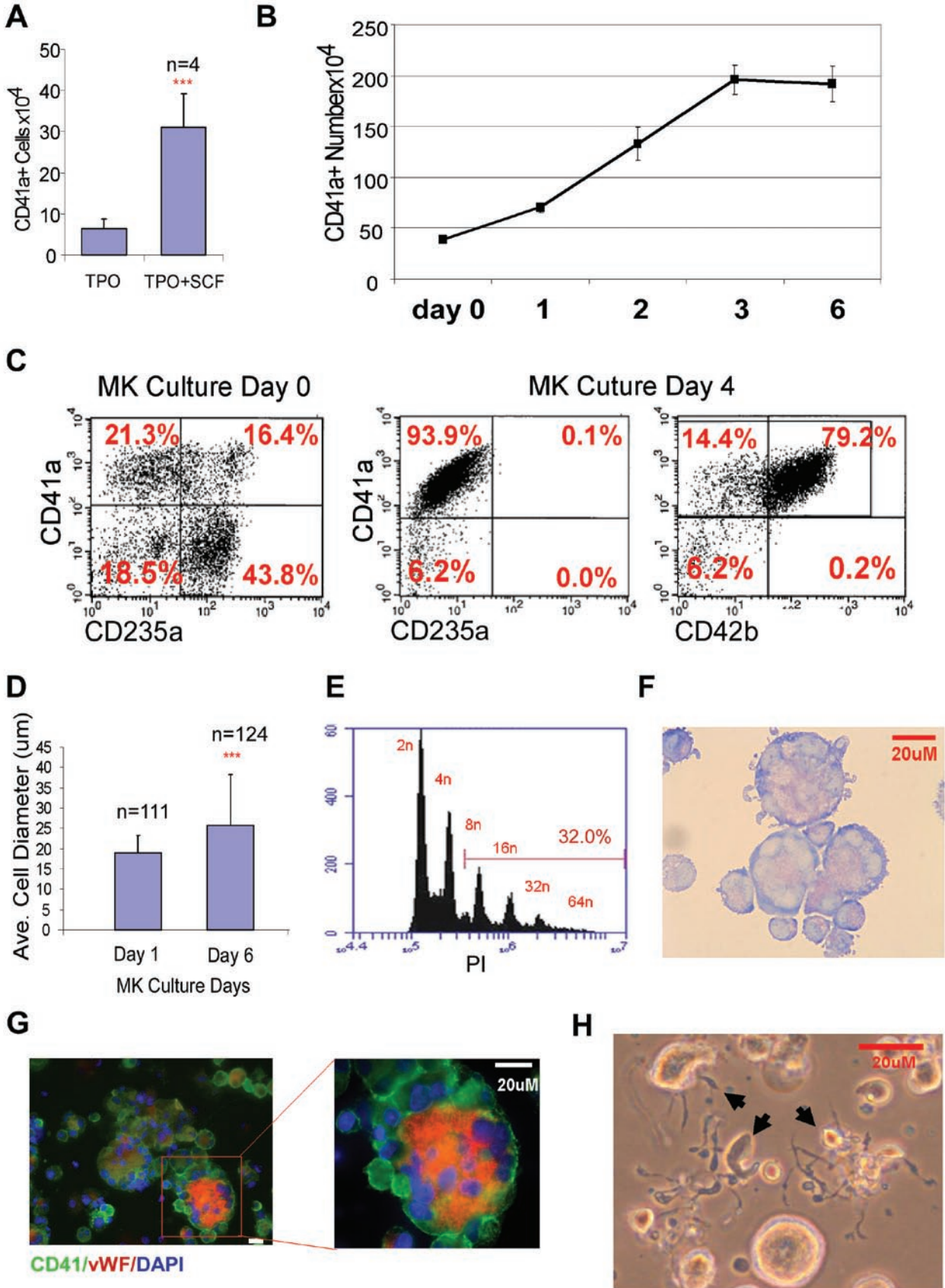
various cytokines and growth factors in a defined culture system. Using serum-free Stemline II as the base medium, we found that a high concentration (50 ng/ml) of TPO was able to support the generation of CD41a+ (GPIIb) cells, although with limited efficiency (Figure 1A). We also observed that most cells died after 6 days of culture if TPO was not supplemented. When TPO was combined with SCF (20 ng/ml), the number of CD41a+ MKs in the differentiation culture significantly increased (Figure 1A, $P < 0.001$, $n = 4$). However, a combination of TPO and SCF with serum or other cytokines such as IL-9, BMP-4, FL, and vascular endothelial growth factor (VEGF) did not increase MK production (Supplementary information, Figure S2). Addition of IL-6, IL-11, and basic fibroblast growth factor (bFGF) individually to medium containing TPO and SCF was able to increase the number of CD41a+ MKs (Supplementary information, Figure S2), but none of these effects was statistically significant (IL-6, $P = 0.110$; IL-11, $P = 0.109$; and bFGF, $P = 0.185$, $n = 5$). Supplementation with all three factors (IL-6, IL-11, and bFGF) together did not improve the outcome either (data not shown). Despite its modest effect, we decided to include IL-11 in our differentiation medium, since it was previously reported to enhance both the expansion and maturation of MKs [19, 20]. On the basis of these results, the MK differentiation medium used in our studies consists of Stemline II supplemented with TPO (50 ng/ml), SCF (20 ng/ml), and IL-11 (20 ng/ml), and is referred to as TSI medium.

Using TSI medium, we were able to achieve a fivefold increase in the number of CD41a+ MKs during a period of 6 days (Figure 1B). During this period, flow cytometry analysis showed a rapid decrease in CD235a+ (glycophorin A+) cells, coupled with a dramatic increase in CD41a+ and CD42b+ (GPIbα) cells. By day 4-6, ~90% of the cells expressed CD41a (Figure 1C, Supplementary information, Figure S3A), and 80% of the cells were also positive for CD42b (Figure 1C). In addition to CD42b, CD42a (GPIX) and CD61 (integrin β3 subunit) were also expressed on the surface of CD41a+ MKs (Supplementary information, Figure S3B). After 4-6 days in the TSI medium, the average cell size significantly increased as well, from 19.0 ± 4.2 μm (mean $\pm$ SD, $n = 111$) in diameter at day 0 to 25.6 ± 12.5 μm ($n = 124$) at day 6 (Figure 1D, $P < 0.001$). By day 6, > 30% of the cells were polyploid with DNA content > 8N (Figure 1E), and > 20% of the cells were > 40 μm in diameter (Figure 1F). Collectively, these results suggest that the TSI culture system facilitates the production of MKs. Consistent with observations in the mouse ESC system [21], most MKs in our cultures were 2N and 4N, suggesting that they were more primitive in nature than what is typically observed *in vivo*. For larger (40-60 μm), more polyploid cells in our cultures, Giemsa and immunofluorescence staining showed characteristic granular accumulation of vWF in the cytoplasm and CD41 staining on the membrane (Figure 1F and 1G), confirming that at least some of the MKs had reached later stages of maturity. Indeed, approximately 1-2% of MKs in our TSI cultures contained proplatelet-like cellular processes by day 4 (Figure 1H).

We have tested the ability of three different hESC lines (HuES-3, MA01, and MA09) to generate MKs in the serum-free and feeder-free TSI conditions. Although variable efficiencies were observed from experiment to

Table 1 Generation of megakaryocytes from human embryonic stem cells (hESC) via hemangioblasts/blast cells

hESC lines	Experiments	Generated CD41+ MK ($\times 10^6$)	Fold expansion from hESCs
HuES-3	1	7	30
	2	15	111
	3	114	95
	4	118	104
MA09	1	22	113
	2	53	29
	3	191	18
	4	604	53
MA01	1	7	65
	2	13	118

CD41+ MK cell counts from cultures were calculated by multiplying total numbers of live cells (trypan blue exclusion) and the percentages of CD41a+ cells (flow cytometry analyses). Total fold expansion from hESCs to MKs were calculated by multiplying the fold expansion at each step through EB, BC and MK cultures, since not all EB cells or BCs were used for subsequent cultures.
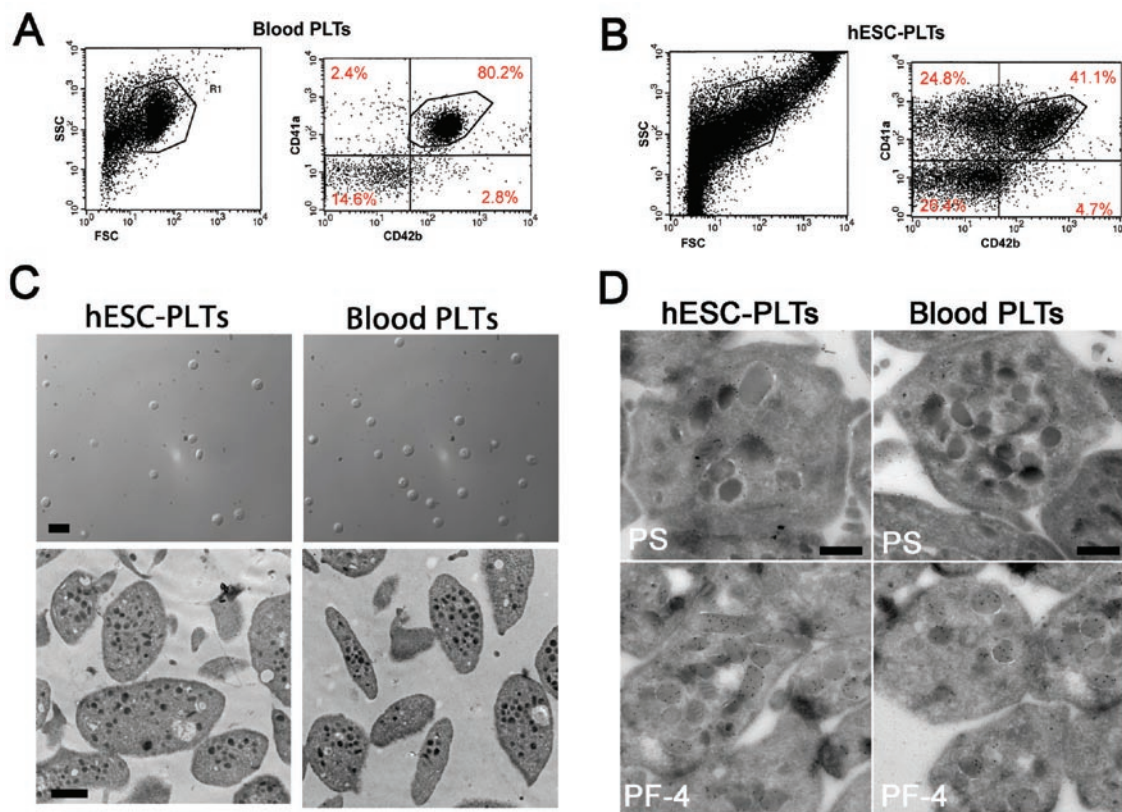
Figure 2 Characterization of platelets generated from human embryonic stem cells (hESC-PLTs). **(A)** The two panels show flow cytometry profiles of forward scatter (FSC) and side scatter (SSC; left), and CD41a and CD42b expression (right) on blood platelets. Approximately 80% of the gated particles express CD41a (*y*-axis) and CD42b (*x*-axis, top right). **(B)** The two panels show a flow cytometry FSC vs SSC profile (left), and CD41a vs CD42b expression (right) on hESC-PLTs. Approximately 30% of hESC-PLTs derived from OP9 feeder co-culture express both CD41a (*y*-axis) and CD42b (*x*-axis, top right). **(C)** Representative microscopic fields of hESC-PLT (top left) and blood platelet (top right) populations examined by differential interference contrast microscopy. Bar = 5 μm. hESc-PLTs are discoid in shape. Thin-section transmission electron microscopy of hESC-PLTs (lower left) and blood platelets (lower right). Bar = 1 μm. **(D)** Expression of P-selectin (PS) and platelet factor 4 (PF-4) on α-granules of blood platelets and hESC-PLTs. Immunogold electron microscopy of ultrathin cryosections showing the localization of P-selectin and PF-4 in resting blood platelets and hESC-PLTs. Bar = 1 μm.

experiment (Table 1), the total expansion of cells from hESCs to CD41a+ MKs ranged from 30- to 111-fold for HuES-3 cells, 65- to 118-fold for MA01 cells, and 18- to 113-fold for MA09 cells. Therefore, our results show approximately 20- to 30-fold greater efficiency in MK production than that of a previous report using both serum and animal feeder cells [15]. For perspective, starting from a single six-well plate of MA09 hESCs ($\approx 1.0 \times 10^7$ cells), $\sim 6 \times 10^8$ CD41a+ MKs were generated (Table 1). With this yield of MKs, ~ 20 standard units of platelets ($\approx 5.5 \times 10^{10}$ platelets/unit) could be produced if *in vitro* thrombopoiesis culture environments were as efficient as those *in vivo* [2, 3].

Generation of functional platelets from hESC-MKs

To determine whether proplatelet-like cellular pro-

cesses observed in our TSI cultures (Figure 1H) reflected generation of hESC-derived platelets (hESC-PLTs), we examined CD41a/CD42b expression by flow cytometry. Using forward and side scatter profiles of human blood platelets to establish proper size gating for hESC-PLTs (Figure 2A), we found that > 30% of hESC-PLTs generated under feeder- and serum-free conditions expressed CD41a, whereas only ~ 5% of CD41a+ hESC-PLTs expressed CD42b (Supplementary information, Figure S4A). Consistent with recent studies showing that the metalloproteinase inhibitor GM6001 significantly increased the expression of CD42b on mouse ESC-derived platelets [22], we found that addition of GM6001 (100 μM) to late stage differentiation cultures tripled the percentage of CD41a+ hESC-PLTs that also expressed CD42b (Supplementary information, Figure

S4B) to ~ 15%, a substantial increase yet still a low total yield. Using the limited number of hESC-PLTs generated under feeder- and serum-free condition, we performed a standard integrin-dependent spreading assay. hESC-PLTs spread on fibrinogen or vWF-coated surfaces (Supplementary information, Figure S5), suggesting that they were functional *in vitro*. Despite the novelty of this entirely serum- and feeder-free system, the low efficiency of functional platelet generation indicates that this method needs further optimization. In an attempt to facilitate thrombopoiesis and generate greater yields of platelets, we amended our differentiation protocol to

include a stroma cell co-culture step after the initial 4-6 days of feeder- and serum-free MK production.

Both OP9 and C3H 10T1/2 mouse stromal cells have been shown to support *in vitro* platelet biogenesis [15, 21, 22]. To determine whether the supportive effects of feeder cells were mediated by secreted factors, we added conditioned medium from OP9 or C3H 10T1/2 cells to our hESC-MK cultures. Stroma-conditioned medium with or without serum had no effect on the generation of functional platelets from our hESC-derived MKs. The addition of fibrinogen and vWF did not enhance platelet production either (data not shown).
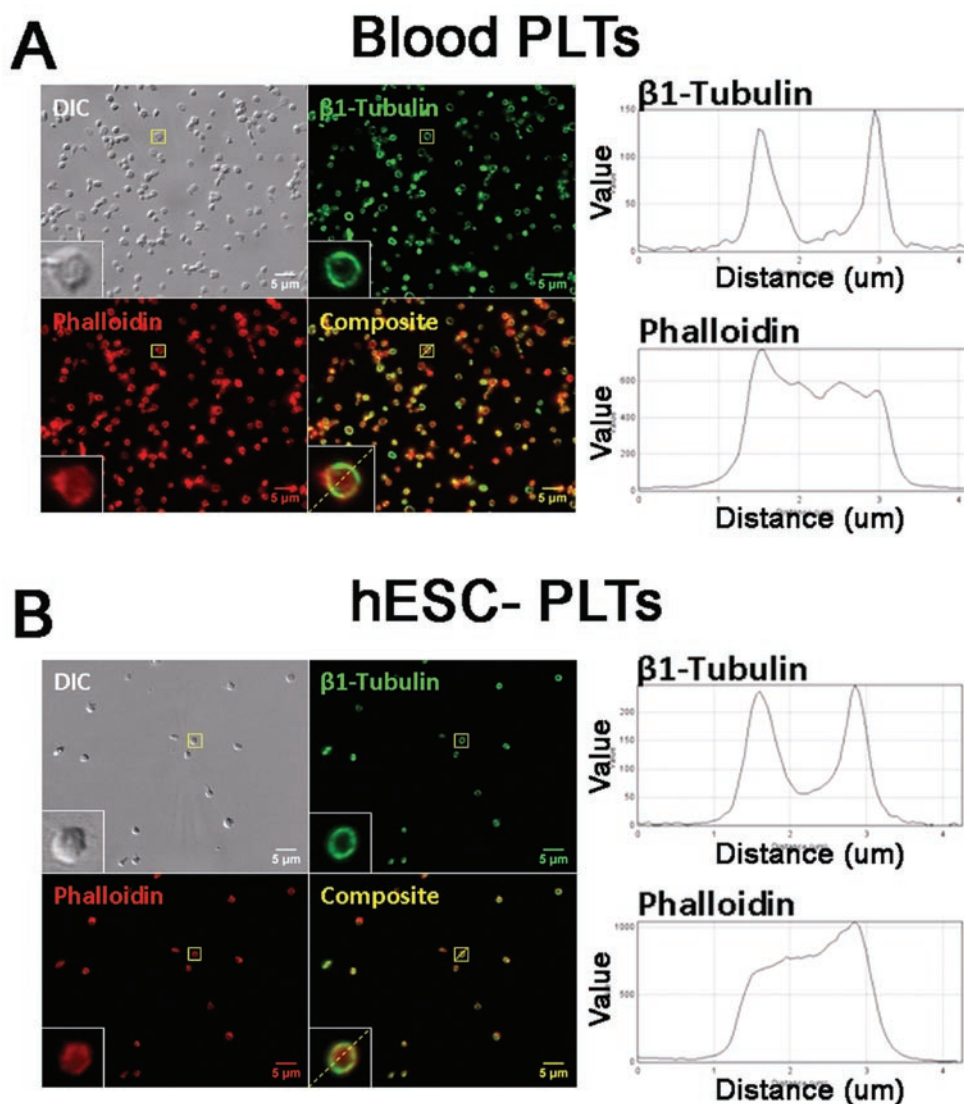

Figure 3 Tubulin and filamentous actin staining in resting blood platelets and hESC-PLTs. Tubulin (green) and filamentous actin staining (red) of resting, blood platelets **(A)** and hESC-PLTs **(B)**. Images are presented as light differential-interference contrast, anti-β1-tubulin staining, phalloidin staining, and an overlay. Plot profiles show distance in microns on the *x*-axis and fluorescence intensity on the *y*-axis. Bar = 5 μm.
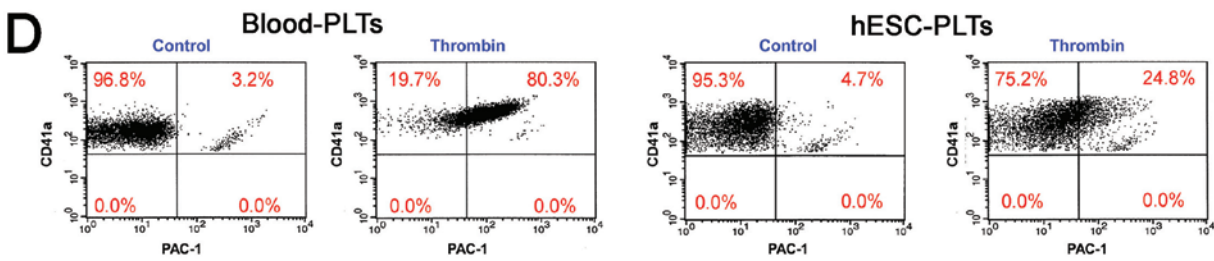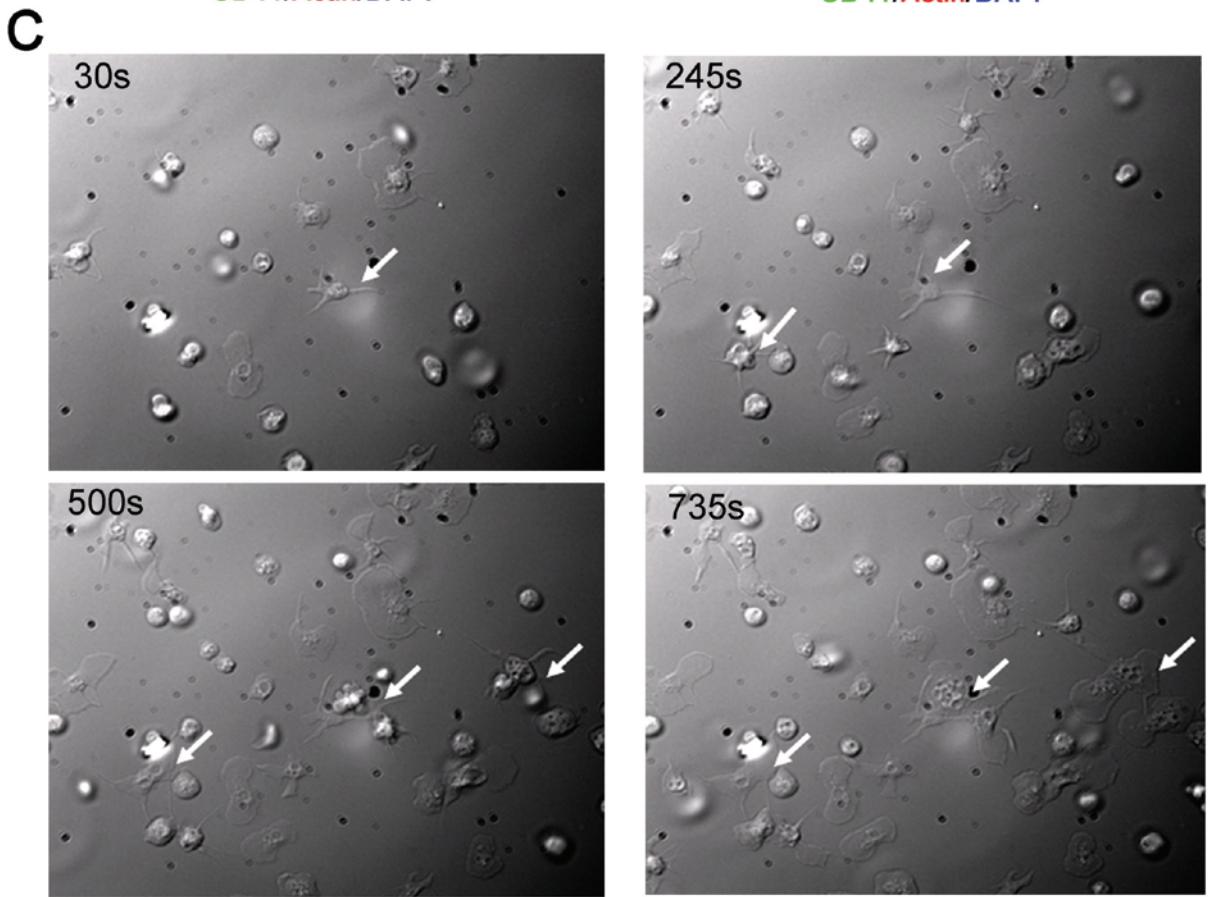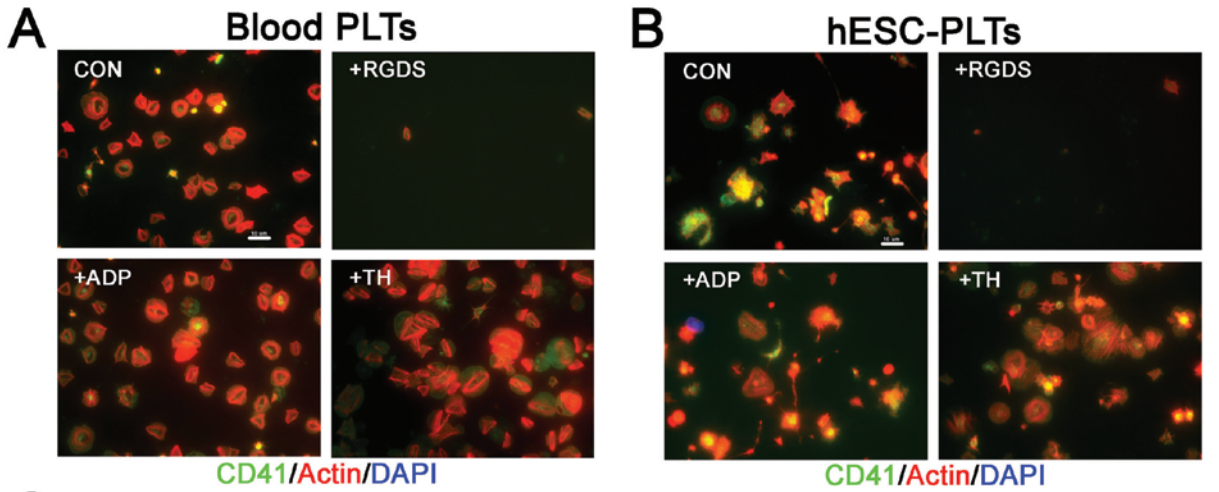
To determine whether direct interaction of MKs with stroma cells is required for efficient platelet biogenesis, hESC-MKs generated from three hESC lines (HuES-3, MA01 and MA09) were harvested from day 4-6 cultures and plated onto mitotically arrested OP9 cells in α-MEM + 15% fetal bovine serum (FBS), 100 ng/ml TPO, 50 ng/ml SCF, and 25 U/ml sodium heparin, as previously described [15]. Cells were grown in stroma co-culture conditions for an additional 4-8 days and the media were collected every 2 days to determine the expression of CD41a/CD42b by flow cytometry. In contrast to hESC-PLTs generated under stroma-free conditions, the majority of CD41a+ hESC-PLTs also expressed CD42b (Figure 2B and Supplementary information, Figure S6) and GM6001 did not significant increase the CD41a/CD42b double-positive population (data not shown).

These hESC-PLTs exhibit each of the characteristic features of blood platelets as demonstrated by differential-interference contrast microscopy. They appeared disc-shaped and measured approximately 2-3 µm in diameter and displayed a key feature of resting platelets – a prominent, circumferential band of microtubules with a diameter similar to that observed in blood platelets (Figure 2C, upper panels, Figure 3). Examination of hESC-PLTs by thin-section electron microscopy demonstrated ultrastructural similarities between hESC-PLTs and blood platelets. hESC-PLTs displayed a smooth contour and contained a normal distribution of the open canalicular system as well as α- and dense granules and other organelles, which are indistinguishable from those isolated from plasma (Figure 2C, lower panels). In addition, hESC-PLTs showed strong expression of P-selectin in the α-granules. Immunogold electron microscopy revealed that expression levels were similar to that observed in blood platelets, and P-selectin was primarily localized to the membranes of α-granules (Figure 2D, upper panels). PF-4 was also localized to α-granules, and gold density was similar to that observed in blood platelets (Figure

2D, lower panels). In summary, hESC-PLTs displayed all of the ultrastructural and morphological criteria that distinguish blood platelets. On average (calculated from six different wells), 6.7 ± 0.4 hESC-PLTs were generated per hESC-MK, the efficiency of which is comparable with that previously reported for *in vitro* platelet production from hESC-MKs [15], but is still much less efficient than that observed *in vivo* [2, 3], suggesting the method needs to be further optimized. We, therefore, used hESC-PLTs generated with OP9 co-culture to perform a variety of functional assays.

We first tested the response of these hESC-PLTs to agonist stimulation. Similar to hESC-PLTs generated under feeder-free TSI conditions (Supplementary information, Figure S5) and normal blood platelets (Figure 4A), hESC-PLTs produced in OP9 co-cultures adhered to and spread on fibrinogen- (Figure 4B) or vWF-coated surfaces (data not shown). An RGDS peptide, which blocks fibrinogen binding to platelet GP IIb/IIIa (αIIbβ3 integrin), abolished the adhesion and spreading of both human blood platelets and hESC-PLTs (Figure 4A and 4B). Live cell microscopy revealed spreading, lamellipodia and filopodia formation, and membrane ruffling of hESC-PLTs; they also spread out and tethered to each other within 10 min after thrombin activation, mimicking the early stage of aggregation, which are typically observed in blood platelets in response to thrombin activation (Figure 4C and Supplementary information, Video S1). In addition, hESC-PLTs adhered to and formed small aggregates on surfaces coated with fibrillar collagen type I under static conditions and treatment with a blocking anti-α2β1 integrin antibody inhibited this adhesion (Supplementary information, Figure S7).

Consistent with previous reports showing a size discrepancy between *in vitro* generated murine and human platelets as compared with their PB counterparts [15, 21-24], we also found that hESC-PLTs were larger and more heterogeneous than human blood platelets in spreading

Figure 4 Functional characterization of hESC-PLTs *in vitro*. **(A)** Human blood platelets and **(B)** hESC-PLTs spread on fibrinogen surface: microtiter chamber slides were coated with 100 µg/ml fibrinogen and human blood platelets treated with vehicle (CON, top left), 1 mM RGDS peptide (+RGDS, top right), 20 µM ADP (+ADP, bottom left) or 1 U/ml of thrombin (+TH, bottom right), were plated and incubated for 90 min. Adherent platelets were stained with Alexa Fluor 568 phalloidin (red), FITC conjugated anti-human CD41a (green) antibodies, and DAPI (blue), and photographed under a fluorescence microscope. Bar = 10 µm. **(C)** Representative images are shown at four time points after thrombin stimulation. Arrows indicate hESC-PLTs spreading, lamellipodia and filopodia formation, membrane ruffling, and some of hESC-PLTs were tethered together. **(D)** The left two panels are representative dot plots for blood platelets binding to FITC-conjugated PAC-1 antibody in the absence (left) and presence (right) of thrombin (1 U/ml). A dramatic increase of FITC-conjugated PAC-1 antibody binding (right shift) is observed for thrombin-treated human platelets as compared with resting controls. The right two panels are representative dot plots for hESC-PLTs binding to FITC-conjugated PAC-1 antibody in the absence (left) and presence (right) of thrombin (1 U/ml). A moderate increase in FITC-conjugated PAC-1 antibody binding (right shift) is observed for thrombin treated hESC-PLTs as compared with resting controls.
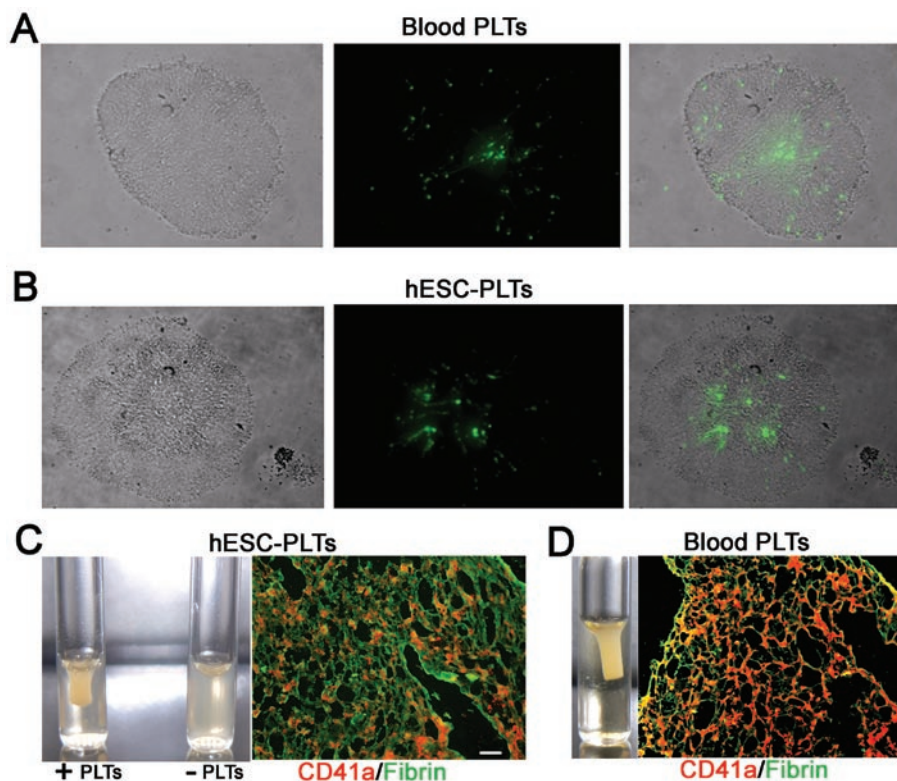
Figure 5 Functional characterization of hESC-PLTs *in vitro*. **(A** and **B)** Aggregation assay: 3×10^5 PKH67 (green) labeled blood platelets **(A)** or 3×10^5 PKH67 labeled hESC-PLTs **(B)** were mixed with unlabeled blood platelets (6×10^7) and thrombin (0.5 U/ml), then stirred to trigger platelet aggregation. Phase contrast (left) and fluorescent images (center) were merged (right) to demonstrate the participation of labeled blood platelets or hESC-PLTs into micro-aggregates. In control experiments, RGDS peptide was added before thrombin stimulation and no aggregation was observed. **(C** and **D)** Clot formation and retraction: **(C)** platelet-depleted human plasma was added with (+PLTs) or without (−PLTs) hESC-PLTs (1.5×10^7/ml), and **(D)** platelet-depleted human plasma was added with human blood platelets (1.5×10^7/ml). Thrombin (2 U/ml) and $CaCl_2$ (10 mM) were then added to the suspensions to induce clot formation/retraction **(C** and **D**, left panels). Clot cryo-sections **(C** and **D**, right panels) were stained with anti-human CD41 (red) and anti-human fibrin (green) antibodies. Images were taken under a fluorescence microscope. No clot formation/retraction was observed without addition of hESC-PLTs **(C**, left panel −PLTs). Bar = 50 μm.

assays. After adherence to bovine serum albumin (BSA)-coated surfaces (Supplementary information, Figure S8), hESC-PLTs had an average diameter of 3.41 ± 1.11 μm (1.82 to 5.76 μm), while blood platelets had an average diameter of 2.76 ± 0.52 μm (1.77 to 4.06 μm). After spreading on fibrinogen surfaces, hESC-PLTs had a diameter of 14.32 ± 4.49 μm (7.37 − 25.79 μm), while blood platelets had a diameter of 9.08 ± 1.85 μm (6.32 − 13.16 μm). Many factors may contribute to this disparity, one of them may be that hESC-PLTs were produced under static conditions, while normal human blood platelets were generated under high shear flow force *in vivo* [25]. Despite this size difference, these results suggest that hESC-PLTs are capable of spreading on a variety of substrate-coated surfaces (collagen, fibrinogen, and vWF) and that their adherence occurs through known receptor-mediated mechanisms (e.g., α2β1 integrin-dependent binding to collagen type I, and αIIbβ3 integrin-dependent binding to fibrinogen).

On activation, platelet αIIbβ3 integrin binding to substrates, such as fibrinogen or vWF, stimulates thrombus formation at the site of vascular injury (reviewed by Coller and Shattil [26]). To determine the extent of functional αIIbβ3 integrin expression that occurs on platelet activation, we performed a binding assay using the PAC-1 monoclonal antibody, a fibrinogen mimetic that only binds to the activated conformation of the αIIbβ3 integrin. In response to thrombin treatment, hESC-PLTs generated from OP9 co-cultured HuES3-MKs showed approximately a fivefold increase in PAC-1 binding as compared with resting controls (Figure 4D, right two panels). In addition to HuES3 cells, hESC-PLTs derived
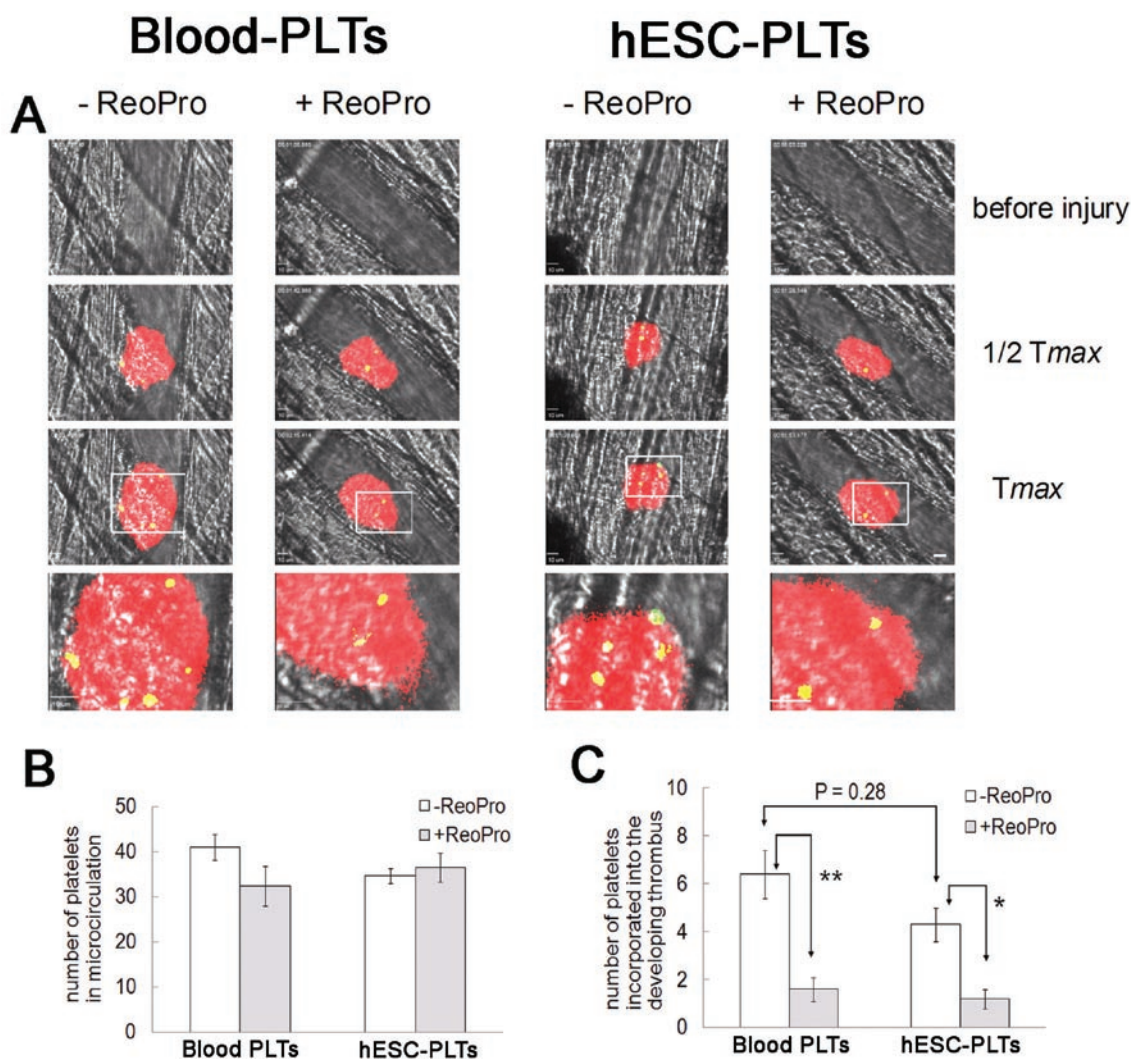
Blood-PLTs

hESC-PLTs

Figure 6 Incorporation of hESC-PLTs into developing mouse platelet thrombi at sites of laser-induced arteriolar injury in living mice. Calcein AM-labeled human blood platelets or hESC-derived platelets, 50-100 μl (5-10 $\times$ 10^5 platelets), were infused through a femoral artery cannulus immediately after laser-induced vascular injury. The developing mouse platelet thrombus was monitored by infusion of Dylight 649-labeled anti-mouse CD42 (0.05 μg/g body weight). After generation of two to three thrombi, the labeled platelets were pretreated with ReoPro, 20 μg for 2 $\times$ 10^6 human platelets in 200 μl, and infused after new vessel injury in the same mouse. Another two to three thrombi were generated to examine incorporation of ReoPro-treated platelets. Data were collected for 3 min following vessel injury. **(A)** Representative fluorescence images are shown at three time points (0, 1/2 T_{max}, and T_{max}) following vascular injury. Magnified images of the area within the white rectangle are shown at the bottom. Bar = 10 μm. **(B and C)** The number of labeled human platelets circulating into the microvessel **(B)** and incorporating into the developing mouse platelet thrombus at the site of vessel injury **(C)** was counted over 3 min after vascular injury. Data represent mean $\pm$ S.E.M. (n = 5-8 thrombi in three mice). *$P < 0.05$ and **$P < 0.01$ vs a control, Student's t-test.

from two clinical grade hESC lines, MA01 and MA09, also expressed CD41a and CD42b antigens (Supplementary information, Figure S6), and bound PAC-1 in response to thrombin stimulation (Supplementary information, Figure S9). Consistent with a previous report [15], PAC-1 binding in response to thrombin was weaker for hESC-PLTs than for blood platelets. In response to thrombin stimulation, PAC-1 binding to blood platelets

increased from 3.2% to 80.3% (Figure 4D, left two panels), while it increased to a lesser degree for hESC-PLTs (4.7% to 24.8%, 1.8% to 18.0%, and 2.0% to 28.6% for hESC-PLTs derived from HuES-3, MA01, and MA09 cells, respectively; Figure 4D, right panels and Supplementary information, Figure S9). The decreased binding capacity of hESC-PLTs may result from multiple factors, one of them is the heterogeneous size distribution of

hESC-PLTs as described above. We also observed that > 80% of blood-PLTs were CD41+/CD42+, while only 40% of hESC-PLTs were CD41+/CD42+ (Figure 2A and 2B). Particles other than CD41+/CD42+ hESC-PLTs and aged hESC-PLTs (collected on days 6 or 7 after plating MKs on OP9 stromal cells) may also contribute to the decreased binding capacity.

hESC-PLTs participate in microaggregate formation and clot formation/retraction

To examine agonist-induced aggregation, hESC-PLTs generated by co-culture with OP9 cells were labeled with green fluorescent dye, mixed with human blood platelets, and stimulated with thrombin. In response to thrombin stimulation under stirring conditions, the labeled hESC-PLTs formed microaggregates together with human blood platelets as confirmed by phase-contrast and fluorescence microscopy. The distribution of hESC-PLTs in these microaggregates was similar to that observed for the same number of fluorescently labeled human blood platelets (Figure 5A and 5B). These results demonstrate that hESC-PLTs together with human blood platelets can form aggregates in response to the appropriate stimulation.

Another important function of activated platelets is to retract fibrin clots [27, 28]. We found that addition of hESC-PLTs to platelet-depleted plasma led to clot formation and retraction in < 30 min following thrombin stimulation (Figure 5C, left panel +PLTs), whereas no clots formed in plain plasma in the absence of platelets even when stimulated with thrombin for > 1 h (Figure 5C, left panel −PLTs). Similar to clot sections formed with human blood platelets (Figure 5D), immunofluorescence microscopy of cryo-sectioned clots derived from hESC-PLTs showed mesh-like networks formed by both fibrin and platelets (CD41a staining, Figure 5C, right panel). These results indicate that hESC-PLTs possess the ability to form compact platelet plugs and to promote fibrin clot formation and retraction.

hESC-PLTs are incorporated into the developing platelet thrombus at the site of laser-induced arteriolar injury in living mice

To determine whether hESC-PLTs can contribute to clot formation *in vivo*, we used a laser-induced vascular injury mouse model coupled with fluorescence intravital microscopy. To monitor mouse platelet thrombus formation, Dylight 649-labeled anti-mouse CD42 antibody was infused into wild-type male mice (C57BL/6, 6-8 week old, $n = 3$) before micropoint laser ablation in the cremaster muscle arteriole. To account for natural variability in thrombus size, 5-8 ablations were made per mouse.

Since anti-CD42 specifically binds to platelets, the size of the mouse platelet thrombus that forms after vessel injury can be measured by the fluorescence intensity of Dylight 649. Consistent with a previous report [29], the median integrated fluorescence signal indicated platelet accumulation began 5-20 s after vascular injury, while half maximal accumulation occurred 49-70 s (1/2 T_{max}) and peak accumulation occurred 70-95 s (T_{max}) after vascular injury (Supplementary information, Figure S10). When 5-10 × 10^5 human peripheral platelets labeled with calcein AM (green) were infused after injury, 41.0 ± 2.8 circulating platelets were detected in the microcirculation near the site of laser-induced vascular injury (Figure 6A and 6B). Among them, 6.4 ± 1.1 platelets incorporated into the developing mouse platelet thrombus within a T_{max} of 73 s (Figure 6A and 6C, Supplementary information, Video S2).

To confirm that the incorporation of human blood platelets into the developing thrombus is mediated by αIIbβ3 integrin, human platelets were pretreated with ReoPro, a Fab fragment of a human-murine chimeric monoclonal antibody that specifically binds to αIIbβ3 integrin on human platelets and inhibits its function [30], before infusion. While the number of circulating platelets was not significantly affected by treatment with ReoPro (32.4 ± 4.4, Figure 6B), the number of human platelets binding to the developing mouse platelet thrombus was significantly reduced to 1.6 ± 0.5 by the time the T_{max} was reached (67 s; Figure 6A and 6C, Supplementary information, Video S3, $P < 0.01$). ReoPro did not affect mouse platelet thrombus formation at the site of vascular injury. These results indicate that human platelets can bind to a mouse platelet thrombus developing at the site of vascular injury and that this binding is mediated by αIIbβ3 integrin.

When 5-10 × 10^5 hESC-PLTs labeled with calcein AM (green) were infused after vascular injury, 34.8 ± 1.7 circulating platelets were detected in the microcirculation (Figure 6A and 6B). Among them, 4.3 ± 0.7 platelets bound to the growing mouse platelet thrombus that formed at the site of vascular injury within the T_{max} of 72 s (Figure 6A and 6C, Supplementary information, Video S4). The difference in number of human blood platelets vs hESC-PLTs incorporating into the developing mouse platelet thrombus was not statistically significant ($P = 0.28$). Similar to blood platelets, pretreatment of hESC-PLTs with ReoPro also significantly reduced the number of platelets that incorporated into the mouse platelet thrombus to 1.2 ± 0.4 by the time the T_{max} (99 s) was reached (Figure 6A and 6C, Supplementary information, Video S5, $P < 0.05$). These results provide the first evidence that hESC-PLTs, such as blood platelets, are func-

tional at the site of vascular injury *in vivo*.

Discussion

High clinical demand for donated platelets has stimulated interest in generating renewable sources of transfusable platelets. Although hESCs could potentially mitigate the need for platelet donation entirely, to do so will require clinically adaptable methods for the *in vitro* differentiation of hESCs into MKs, and their maturation and fragmentation to produce high yields of functional platelets. In this study, we demonstrate an efficient method for the differentiation of hESCs into MKs, and that the platelets subsequently generated are functionally similar to normal blood platelets *in vitro* as well as in living animals. This system is both amenable to large-scale production efforts and provides the first known evidence for the *in vivo* functionality of hESC-derived platelets.

Two previous studies [14, 15] have demonstrated the feasibility of the first step (generation of MKs from hESCs), but also highlight critical issues that need to be resolved. In both studies, animal stromal cells and animal serum were required throughout the MK generation period, making these methods difficult to adapt for clinical production. In addition, the yield of MKs in these systems is low. Gaur *et al.* [14] reported the generation of less than one (0.1 to 0.4) MK from each hESC. Although Takayama *et al.* [15] improved on this yield (generating two to five MKs per hESC), the use of handpicking hES-sacs significantly hinders the ability to translate this to a clinically relevant scale. The present system, which uses hemangioblast/BC intermediates, is exponentially more efficient in generating CD41a+ MKs than previous methods, and can be carried out under defined serum- and animal feeder-free conditions.

Although the maturation and fragmentation of MKs *in vivo* leads to the generation and release of platelets, this thrombopoietic process has proven extremely difficult to recapitulate *in vitro*. On generating MKs from hESCs, Takayama *et al.* [15] have been the only group to report the subsequent production of platelets from hESC-derived MKs. By continuing to grow their MKs on animal feeder cells, platelets were subsequently produced and shown to be functional using *in vitro* methods. Although we also found that efficient platelet generation from MKs required conventional stroma co-culture, importantly, we provide the first *in vivo* evidence for human hESC-PLTs functionality. *In vitro*, our hESC-PLTs showed the ability to adhere and spread on fibrinogen-, vWF-, and type I collagen-coated surfaces (Figure 4B and 4C, Supplementary information, Figure S7 and Video S1) and to aggregate when stimulated with physiological agonists

(Figure 5B). Moreover, our results show that hESC-PLTs can retract fibrin clots through a predicted integrin-mediated retractile motion (Figure 5C). Since clot retraction promotes wound healing, and thus long-term vascular health, it was important to verify this critical feature of platelet functionality.

Thrombus formation *in vivo* is a rapid and highly dynamic process involving a large number of signaling pathways, enzymatic cascades, and the interplay of various protein components. In the past decade, several experimental models have been established to investigate thrombus formation in mice, including the laser-injury thrombosis model (see reviews by Day *et al.* [31], Sachs and Nieswandt [32], and Yu *et al.* [33]). By inducing natural platelet thrombus formation at the site of vascular injury in as little as 5-20 s, this system enabled us to monitor the real-time incorporation of human platelets or hESC-PLTs into a newly forming thrombus before they could be cleared from the microcirculation. We found that hESC-PLTs, such as human blood platelets, incorporated into the developing mouse platelet thrombus through an αIIbβ3 integrin-dependent mechanism. The number of hESC-PLTs interacting with the mouse thrombus was slightly lower than that of human blood platelets (Figure 6C). While this difference was not statistically significant, we hypothesize that reduced PAC-1 binding of activated hESC-PLTs compared with that of activated human blood platelets (Figure 4D and Supplementary information, Figure S9) may be partially responsible. One other contributing factor may be the larger and more heterogeneous size of hESC-PLTs than human blood platelets. While normal human blood platelets are generated under high shear flow force *in vivo* [25], platelets collected from *in vitro* cultures are produced under static conditions, and this difference in their biogenesis could contribute to subtleties in feature and function. Furthermore, the aged hESC-PLTs collected on days 6 or 7 after plating MKs on OP9 stromal cells may be another contributing factor.

In conclusion, the study described here represents an important step in developing a renewable, donorless source of transfusable platelets. In addition to reducing dependence on animal serum and stroma, thus making the process more amenable to clinical translation, we have provided the first *in vivo* evidence of hESC-PLT functionality. Megakaryopoiesis and thrombopoiesis are highly complex processes, with sophisticated reorganization of membranes and microtubules as well as precise distributions of granules and organelles [25]. The ability to generate MKs under serum- and feeder-free conditions and to examine platelet functionality *in vivo* should aid in the screening of factors to further optimize *in vitro* cul-

ture methods. Importantly, by using induced pluripotent stem cells [34-37], it may be possible to adapt these differentiation protocols to produce patient-specific platelets for transfusion-dependent patients who develop platelet alloimmunity.

Materials and Methods

Generation of MKs and platelets from hESCs via hemangioblasts/BCs

Hemangioblast/BC generation from hESC lines (HuES-3, MA01 and MA09) was performed as previously reported [16, 17]. IL-6, IL-9, IL-11, basic FGF, VEGF, TPO, and SCF were obtained from Peprotech, BMP-4 was obtained from Stemgent. BCs from day 6 to 8 cultures were purified and plated (1 to 5×10^5/ml) in "TSI medium" which consisted of Stemline II (Sigma-Aldrich, St Louis, MO, USA) supplemented with 50 ng/ml TPO, 20 ng/ml SCF, and 20 ng/ml IL-11 (all from Peprotech) to induce BC differentiation toward MKs. Half of the MK culture medium was replaced with fresh TSI medium every 2 or 3 days. Platelet generation from MKs was performed under either stroma feeder-free or stroma feeder co-culture conditions, as indicated. For feeder-free platelet generation, MKs from day 4 to 6 cultures were simply maintained in TSI medium for an additional 4-8 days, whereupon platelets were collected intermittently for analysis. In some experiments, GM6001 (100 µM) was added to late stage differentiation cultures. For feeder co-culture experiments, OP9 or C3H 10T1/2 stromal cells were maintained in OP9 culture medium (α-MEM with 15% Hyclone fetal bovine serum). Confluent OP9 or C3H 10T1/2 cells were treated with 100 ng/ml mitomycin-C the day before co-culture, gently washed twice with PBS and allowed to recover overnight in OP9 culture medium. MKs from day 4 to 6 cultures were collected and replated onto mitotically inactivated OP9 or C3H 10T1/2 stromal cells in OP9 culture medium plus 100 ng/ml TPO, 50 ng/mlSCF, and 25 U/ml sodium heparin, as previously described [15]. Platelets were intermittently collected 4 to 8 days later for various analyses.

Hematopoietic colony formation assays

Megacult-C Kit (Stem Cell Technology, Canada) was used for CFU-MK colony formation assays. After 10 day of plating, CFU-MK cultures were dehydrated, fixed, and stained with anti-CD41 antibody as suggested by the manufacturer. CFU-MK colonies were scored according to the standards provided in the Megacult-C protocol.

Flow cytometry analysis

Cells from blast cultures or MK cultures were monitored routinely by flow cytometry on a FACSCalibur (Becton Dickinson) or Accuri C6 Cytometer (Accuri Cytometers). Fluorochrome-conjugated antibodies for lineage markers, CD41a, CD42a, CD42b, and CD235a (BD Biosciences) were used to characterize MK and erythroid lineages. Antibodies were freshly prepared (1:100 dilution for CD42a and CD42b antibodies; 1:250 dilution for CD41a antibody; 1:2 000 for CD235a antibody) in PBS buffer with 5% FBS. Typically 1 to 2×10^5 cells were used for antibody labeling. Cells were stained in a 100 µl antibody cocktail for 1 h on ice, then washed twice with buffer, and resuspended in 250 µl

buffer supplemented with 1 µg/ml propidium iodide. To detect the expression level of HLA-ABC, platelets were incubated with a fluorescein isothiocyanate (FITC)-conjugated anti-human HLA-ABC antibody or FITC-conjugated mouse immunoglobulin G (IgG) as a control. The samples were then processed on a FACSCalibur and data was analyzed using Cellquest Pro (BD Biosciences) or Flowjo (Tree Star) software.

DNA content analysis

For polyploidy analysis, cells from day 4-6 MK cultures were fixed in 70% ethanol for 2 h. Cells were then washed once in PBS buffer before staining with 20 µg/ml propidum iodide (Sigma-Aldrich), 20 µg/ml RNase A (Sigma-Aldrich) in PBS buffer overnight at 4 °C. Cellular DNA content was analyzed on an Accuri C6 flow cytometer.

Cytospin preparation, Giemsa staining, and immunofluorescence

Cells (1 to 2×10^4) from either blast cultures or MK cultures were cytospun onto polylysine-coated slides (Wessco). Slides were either used for Wright-Giemsa (Sigma-Aldrich) staining or immunofluoroscence. All incubations were performed at room temperature. Cells were blocked with animal-free blocker (Vector Laboratories) for 30 min, incubated with primary antibodies for 1 h, and then washed three times with PBS. For MK identification, primary antibodies include anti-CD41 (1:100; Dako cytomation, Carpinteria, CA, USA) and anti-vWF (1:200, Dako). Cells were incubated with secondary antibodies (1:200 each) for 30 min in the dark, and washed again three times in PBS. DAPI (1 µg/ml) in PBS was used to stain nuclei for 5 min followed by three more PBS washes. Slides were then mounted and examined under Olympus BX51 fluorescence microscope (MVI, Avon, MA, USA). Fluorescent images were captured using a QICAM Fast camera (QImaging, Surrey, BC, Canada) and analyzed with Q Capture Pro version 5.1 software (Media Cybernetics, Bethesda, MD, USA). Phase contrast live cell images were captured using a Nikon microscope, PAXCAM digital camera and PAX-it software.

Preparation of human blood platelets and hESC-derived platelets

Human platelets were isolated as previously described [38]. Briefly, human platelet-rich plasma was prepared by centrifugation of sodium citrate-treated human blood at $200 \times g$ for 20 min. The supernatant was collected and centrifuged at $700 \times g$ for 10 min in the presence of 0.5 µM PGE1 and 10% sodium citrate buffer. The pellet was resuspended with HEPES-Tyrode buffer (12 mM NaHCO$_3$, 138 mM NaCl, 5.5 mM Glucose, 2.9 mM KCl, 0.42 mM NaHPO$_4$, 10 mM HEPES, 1 mM CaCl$_2$, 1 mM MgCl$_2$) containing 0.15 µM PGE1, and centrifuged at $800 \times g$ for 5 min. The pellet was resuspended in RPMI1640 containing 0.1% fatty acid-free bovine serum albumin, 2 mM CaCl$_2$, and 1 mM MgCl$_2$. Final suspensions of washed platelets were adjusted to 1×10^7 platelets/ml. Approval to obtain blood samples was obtained from the University of Illinois-Chicago review board. Informed consent was provided according to the Declaration of Helsinki. In some experiments, human blood samples were also obtained from a commercial source (AllCells, Emeryville, CA, USA). For hESC-PLTs, culture media containing hESC-PLTs were gently collected with apyrase (1 U/ml) and EDTA (5 mM; Sigma-Aldrich) being

added to prevent platelet activation. hESC-PLTs were enriched and washed as described above. Washed blood platelets and hESC-PLTs were incubated at 37 °C for 0.5-2 h before functional assays were performed.

Differential interference contrast and electron microscopy analyses

To study cell shape, hESC-PLTs were fixed with 1% glutaraldehyde in platelet buffer for 20 min, moved to a coverslip chamber, and viewed with a 63× differential interference contrast objective. Images were obtained using a cooled CCD camera with Metamorph software (Universal Imaging). Anti-tubulin immunofluorescence microscopy was performed as described previously [39]. Images were analyzed using the Metamorph image analysis software (Molecular Devices, Sunnyvale, CA, USA). Plot profiles were generated using ImageJ (NIH, http://rsb.info.nih.gov/ij/). Thin-section electron microscopy was carried out as previously described [40]. Anti-P-selectin and anti-PF-4 immunogold electron microscopy was carried out as described previously [41]. Live cell video microscopy of platelets undergoing activation was performed using previously described methods [42]. Images of spreading platelets were captured every 5 s for 10 min.

Platelet spreading on various substrates

Spreading and adhesion of blood platelets and hESC-PLTs on immobilized surfaces of fibrinogen, vWF, type I collagen, and BSA were performed as reported [21, 43]. Chamber slides with microtiter wells (Nalgen Nunc, Rochester, NY, USA) or coverslips were coated with 100 µg/ml fibrinogen or vWF (30 µg/ml; Sigma-Aldrich), acid-soluble fibrillar type I collagen (20 µg/ml, Millipore) or 1% fatty acid-free BSA (Sigma-Aldrich) in 0.1 M NaHCO$_3$ (pH 8.3) at 4 °C overnight. Washed human blood platelets or hESC-PLTs (1×10^7/ml) were allowed to adhere and spread on protein-coated wells at 37 °C for 90 min. In some experiments, platelets were preincubated with an αIIbβ3 integrin antagonist (RGDS peptide) for 5 min before loading. In other experiments, platelets were mixed with ADP (20 µM) or thrombin (1 U/ml; Sigma-Aldrich), or were pretreated with 20 µg/ml of isotype control mouse IgG1 or a blocking anti-α2β1 antibody (BHA2.1, Millipore) for collagen-coated surfaces, and immediately loaded onto fibrinogen-, vWF-, or collagen-coated wells, as indicated. After washing with PBS buffer, cells were fixed, permeabilized, and stained with Alexa Fluor 568 phalloidin (Molecular Probes, Eugene, OR, USA), FITC conjugated anti-human CD41a antibody (Dako cytomation) and DAPI. Adherent platelets were viewed with an Olympus BX51 fluorescence microscope using a PlanApo lens at 100×/1.40 oil objective, or using a Nikon microscope (E400) equipped with a 100×/1.3 NA oil objective. Images were acquired using a QICAM Fast camera and processed with Q Capture version 5.1 software, or using a CoolSNAP camera (ES2, 1 392 × 1 040 imaging pixels, Photometrics, Tucson, AZ, USA), and NIS Element software (Advanced, v3.1).

Formation of platelet microaggregates

Washed human blood platelets and hESC-PLTs were resuspended in modified Tyrode buffer and labeled with a PKH67 Green Fluorescent Cell Linker (10 µM, Sigma-Aldrich). Human blood platelets (6×10^7) were mixed with fluorescence-labeled human blood platelets (3×10^5) or hESC-PLTs (3×10^5) in a 450 µl cu-

vette (Chronolog, Havertown, PA, USA), treated with thrombin (0.5 U/ml) and stirred at 1 200 r.p.m. at 37 °C to trigger platelet aggregation. In control experiments, platelets were preincubated with RGDS peptide at 37 °C for 5 min before the addition of thrombin, and then aggregation assays were performed as above. Platelet microaggregates in 50 µl buffer were spread onto glass slides and visualized under an Olympus BX51 fluorescence microscope.

PAC-1 binding assay

Human blood platelets or hESC-PLTs with or without thrombin stimulation (1 U/ml, incubation at room temperature for 20 min) were stained with APC-conjugated CD41a, PE-conjugated CD42b, and FITC-conjugated PAC-1 antibodies in modified Tyrode's buffer. The samples were then analyzed using a FACSCalibur. Forward vs side scatter gating was determined using human blood platelets as controls. Flow cytometry data was analyzed using Cellquest Pro or Flowjo software.

Clot formation and retraction

Human blood platelets or hESC-PLTs (approximately 1.5×10^7/ml) were resuspended in 50 µl platelet-depleted plasma in a siliconized glass tubes (Kimble Chase, Vineland, NJ, USA). Thrombin (2 U/ml) was added to the cells to induce clot formation and retraction. The clots were allowed to retract at 37 °C for 1 h and photographed. Clots were embedded in Tissue-Tek OCT compound and Tissue-Tek Cryomolds (Sakura Finetek, Torrance, CA, USA), and then frozen in dry ice. 10 µm clot sections were made using a cryostat microtome Microm HM 560 (Thermo Scientific, Kalamazoo, MI, USA). Slides were fixed with methanol/acetone (1:3) for 30 min, washed with PBS, and permeabilized with 0.1% Triton X-100, 0.1 M Tris, 10 mM EGTA, 0.15 NaCl, 5 mM MgCl$_2$, and 1% BSA, pH 7.5. After blocking with 5% BSA and washing with PBS, sections were immunostained with rabbit anti-human integrin αIIb (clone H-160) and mouse anti-human fibrin (clone UC45) antibodies (Santa Cruz Biotech, Santa Cruz, CA, USA). Sections were then incubated for 1 h in a 1:200 dilution of rhodamine-anti-rabbit IgG and FITC-anti-mouse IgM (Jackson ImmunoResearch Laboratory, Bar Harbor, ME, USA). Images were taken as described above.

Intravital microscopy

Male wild-type mice (C57BL/6, 6-8 week old) were purchased from the Jackson ImmunoResearch Laboratory. The University of Illinois Institutional Animal Care and Use Committee approved all animal care and experimental procedures. Wide field, multichannel intravital microscopy of the cremaster muscle microcirculation was performed as previously described [29, 44]. Male mice were anesthetized by an intraperitoneal injection of ketamine (125 mg/kg, Bedford Laboratories, Bedford, OH, USA) and xylazine (25 mg/kg, Akorn, Decatur, IL, USA). A tracheal tube was inserted and the mouse was placed on a thermo-controlled blanket (37 °C). To maintain anesthesia, 50 µl of the ketamine and xylazine solution was administered every 30 min through a cannulus placed in the jugular vein. An additional cannulus, filled with saline containing 10 U/ml heparin, was placed in the femoral artery. After the scrotum was incised, the cremaster muscle was carefully exteriorized onto an intravital microscopy tray so that it could be monitored without detaching it from the body. The muscle preparation was superfused with thermo-controlled (37 °C) and aerated (95% N$_2$,

5% CO_2) bicarbonate-buffered saline throughout the experiment.

The cremaster muscle arteriolar wall was injured by laser ablation using a Micropoint Laser System (Photonics Instruments, South Windsor, CT, USA) as described previously [29]. The developing mouse platelet thrombus was monitored by infusion of Dylight 649 (red)-labeled anti-mouse CD42 (Emfret Analytics, 0.05 µg/g body weight). One or two pulses ablated an inside vessel wall to stimulate platelet thrombus formation. To determine if they could incorporate into the developing mouse platelet thrombus, human blood platelets or hESC-PLTs, labeled with calcein AM, (green, Invitrogen; 50-100 µl per 5-10 × 10⁵ platelets) were infused through a femoral artery cannulus while the mouse platelet thrombus (red) was growing. Multiple thrombi were studied in one mouse, with each new ablation being made upstream of the earlier one to avoid any previous thrombus contribution to the newly forming one. Labeled human platelets, which had been previously infused into a mouse were allowed to completely clear the microcirculation before a new vascular ablation was made. To determine whether their incorporation was dependent on $\alpha IIb\beta3$ integrin signaling, human blood platelets, or hESC-PLTs were pretreated with ReoPro (20 µg for 2×10^6 human platelets in 200 µl, Centocor) before infusion. ReoPro is a Fab fragment of a human-murine chimeric monoclonal antibody that specifically binds to $\alpha IIb\beta3$ integrin on human platelets and inhibits its function [30]. In general, two to three ablation-induced thrombi were allowed to form in each mouse to establish human platelet incorporation parameters without ReoPro. Then, another two to three thrombi were generated to examine incorporation of the ReoPro-treated human platelets. Human blood platelets and hESC-PLTs were studied in different mice. Microvessel data were obtained using an Olympus BX61WI microscope with a 60× objective. Digital images were captured with a high-speed digital camera (Hamamatsu C9300) through an intensifier (Video Scope International, Dulles, VA, USA). Fluorescence images were analyzed using Slidebook v5.0 (Intelligent Imaging Innovations, Denvor, CO, USA). Fluorescence images were captured at exposure times of 10-100 milliseconds and bright field images were captured with exposure times of 20 milliseconds. Data were collected for 3 min following vessel wall injury. To simplify the image analysis, the dynamic range of the intensity of each pseudocolor was binarized. The number of human platelets circulating in the microvessel and incorporated into the developing mouse platelet thrombus at the site of vessel injury was counted over 3-4 min after vascular injury. The kinetics of mouse platelet thrombus formation were analyzed by determining median fluorescence intensity values of anti-CD42 antibody over time in approximately five to eight thrombi in three mice [29]. T_{max} and $1/2$ T_{max} were defined as the time points at which the mouse platelet thrombus had reached its maximum and 1/2 maximum size, respectively.

Statistical analysis

Data were statistically analyzed by Student's *t*-test for comparison of two groups using GraphPad Prism (GraphPad Software). Differences were considered significant at $P < 0.05$.

Acknowledgments

References

1   Reems JA, Pineault N, Sun S. *In vitro* megakaryocyte production and platelet biogenesis: state of the art. *Transfus Med Rev* 2010; **24**:33-43.

2   Kaufman RM, Airo R, Pollack S, *et al*. Circulating megakaryocytes and platelet release in the lung. *Blood* 1965; **26**:720-731.

3   Long MW. Megakaryocyte differentiation events. *Semin Hematol* 1998; **35**:192-199.

4   Kaushansky K. Historical review: megakaryopoiesis and thrombopoiesis. *Blood* 2008; **111**:981-986.

5   Wang X, Crispino JD, Letting DL, *et al*. Control of megakaryocyte-specific gene expression by GATA-1 and FOG-1: role of Ets transcription factors. *EMBO J* 2002; **21**:5225-5234.

6   Gaines P, Geiger JN, Knudsen G, *et al*. GATA-1- and FOG-dependent activation of megakaryocytic α IIB gene expression. *J Biol Chem* 2000; **275**:34114-34121.

7   Shivdasani RA, Fujiwara Y, McDevitt MA, *et al*. A lineage-selective knockout establishes the critical role of transcription factor GATA-1 in megakaryocyte growth and platelet development. *EMBO J* 1997; **16**:3965-3973.

8   Schmitt A, Guichard J, Masse JM, *et al*. Of mice and men: comparison of the ultrastructure of megakaryocytes and platelets. *Exp Hematol* 2001; **29**:1295-1302.

9   Deutsch VR, Tomer A. Megakaryocyte development and platelet production. *Br J Haematol* 2006; **134**:453-466.

10 Kosaki G. *In vivo* platelet production from mature megakaryocytes: does platelet release occur via proplatelets? *Int J Hematol* 2005; **81**:208-219.

11 Patel SR, Hartwig JH, Italiano JE Jr. The biogenesis of platelets from megakaryocyte proplatelets. *J Clin Invest* 2005; **115**:3348-3354.

12 Guerriero R, Mattia G, Testa U, *et al*. Stromal cell-derived factor 1α increases polyploidization of megakaryocytes generated by human hematopoietic progenitor cells. *Blood* 2001; **97**:2587-2595.

13 Matsunaga T, Tanaka I, Kobune M, *et al*. *Ex vivo* large-scale generation of human platelets from cord blood CD34+ cells. *Stem Cells* 2006; **24**:2877-2887.

14 Gaur M, Kamata T, Wang S, *et al*. Megakaryocytes derived from human embryonic stem cells: a genetically tractable system to study megakaryocytopoiesis and integrin function. *J Thromb Haemost* 2006; **4**:436-442.

15 Takayama N, Nishikii H, Usui J, *et al*. Generation of functional platelets from human embryonic stem cells *in vitro* via ES-sacs, VEGF-promoted structures that concentrate hematopoietic progenitors. *Blood* 2008; **111**:5298-5306.

16 Lu SJ, Feng Q, Caballero S, *et al*. Generation of functional hemangioblasts from human embryonic stem cells. *Nat Meth-*

ods 2007; **4**:501-509.

17 Lu SJ, Luo C, Holton K, *et al*. Robust generation of hemangioblastic progenitors from human embryonic stem cells. *Regen Med* 2008; **3**:693-704.

18 Lu SJ, Feng Q, Park JS, *et al*. Biologic properties and enucleation of red blood cells from human embryonic stem cells. *Blood* 2008; **112**:4475-4484.

19 Taguchi K, Saitoh M, Arai Y, *et al*. Disparate effects of interleukin 11 and thrombopoietin on megakaryocytopoiesis *in vitro*. *Cytokine* 2001; **15**:241-249.

20 Philipp CS, Remmler J, Zucker-Franklin D. The effects of Mpl-ligand, interleukin-6 and interleukin-11 on megakaryocyte and platelet α-granule proteins. *Thromb Haemost* 1998; **80**:968-975.

21 Fujimoto TT, Kohata S, Suzuki H, *et al*. Production of functional platelets by differentiated embryonic stem (ES) cells *in vitro*. *Blood* 2003; **102**:4044-4051.

22 Nishikii H, Eto K, Tamura N, *et al*. Metalloproteinase regulation improves *in vitro* generation of efficacious platelets from mouse embryonic stem cells. *J Exp Med* 2008; **205**:1917-1927.

23 Cramer EM, Norol F, Guichard J, *et al*. Ultrastructure of platelet formation by human megakaryocytes cultured with the Mpl ligand. *Blood* 1997; **89**:2336-2346.

24 Robert A, Boyer L, Pineault N. Glycoprotein Ibα receptor instability is associated with loss of quality in platelets produced in culture. *Stem Cells Dev* 2010 Sep 15. doi:10.1089/scd.2010.0041

25 Junt T, Schulze H, Chen Z, *et al*. Dynamic visualization of thrombopoiesis within bone marrow. *Science* 2007; **317**:1767-1770.

26 Coller BS, Shattil SJ. The GPIIb/IIIa (integrin αIIbβ3) odyssey: a technology-driven saga of a receptor with twists, turns, and even a bend. *Blood* 2008; **112**:3011-3025.

27 Chen YP, O'Toole TE, Ylanne J, *et al*. A point mutation in the integrin β3 cytoplasmic domain (S752→P) impairs bidirectional signaling through αIIbβ3 (platelet glycoprotein IIb-IIIa). *Blood* 1994; **84**:1857-1865.

28 Jirouskova M, Smyth SS, Kudryk B, *et al*. A hamster antibody to the mouse fibrinogen γ chain inhibits platelet-fibrinogen interactions and FXIIIa-mediated fibrin cross-linking, and facilitates thrombolysis. *Thromb Haemost* 2001; **86**:1047-1056.

29 Cho J, Furie BC, Coughlin SR, *et al*. A critical role for extracellular protein disulfide isomerase during thrombus formation in mice. *J Clin Invest* 2008; **118**:1123-1131.

30 Coller BS. Anti-GPIIb/IIIa drugs: current strategies and future directions. *Thromb Haemost* 2001; **86**:427-443.

31 Day SM, Reeve JL, Myers DD, *et al*. Murine thrombosis

models. *Thromb Haemost* 2004; **92**:486-494.

32 Sachs UJ, Nieswandt B. *In vivo* thrombus formation in murine models. *Circ Res* 2007; **100**:979-991.

33 Furie B, Furie BC. *In vivo* thrombus formation. *J Thromb Haemost* 2007; **5** Suppl 1:12-17.

34 Yu J, Vodyanik MA, Smuga-Otto K, *et al*. Induced pluripotent stem cell lines derived from human somatic cells. *Science* 2007; **318**:1917-1920.

35 Takahashi K, Tanabe K, Ohnuki M, *et al*. Induction of pluripotent stem cells from adult human fibroblasts by defined factors. *Cell* 2007; **131**:861-872.

36 Yu J, Hu J, Smuga-Otto K, *et al*. Human induced pluripotent stem cells free of vector and transgene sequences. *Science* 2009; **324**:797-801.

37 Kim D, Kim CH, Moon JI, *et al*. Generation of human induced pluripotent stem cells by direct delivery of reprogramming proteins. *Cell Stem Cell* 2009; **4**:472-476.

38 Cho J, Mosher DF. Enhancement of thrombogenesis by plasma fibronectin cross-linked to fibrin and assembled in platelet thrombi. *Blood* 2006; **107**:3555-3563.

39 Patel-Hett S, Richardson JL, Schulze H, *et al*. Visualization of microtubule growth in living platelets reveals a dynamic marginal band with multiple microtubules. *Blood* 2008; **111**:4605-4616.

40 Richardson JL, Shivdasani RA, Boers C, *et al*. Mechanisms of organelle transport and capture along proplatelets during platelet production. *Blood* 2005; **106**:4066-4075.

41 Italiano JE Jr, Richardson JL, Patel-Hett S, *et al*. Angiogenesis is regulated by a novel mechanism: pro- and antiangiogenic proteins are organized into separate platelet α granules and differentially released. *Blood* 2008; **111**:1227-1233.

42 Barkalow KL, Falet H, Italiano JE Jr, *et al*. Role for phosphoinositide 3-kinase in Fcγ RIIA-induced platelet shape change. *Am J Physiol Cell Physiol* 2003; **285**:C797-C805.

43 Cho J, Mosher DF. Impact of fibronectin assembly on platelet thrombus formation in response to type I collagen and von Willebrand factor. *Blood* 2006; **108**:2229-2236.

44 Falati S, Gross P, Merrill-Skoloff G, *et al*. Real-time *in vivo* imaging of platelets, tissue factor and fibrin during arterial thrombus formation in the mouse. *Nat Med* 2002; **8**:1175-1181.

(**Supplementary information** is linked to the online version of the paper on the *Cell Research* website.)